JOURNAL OF CHEMICAL & ENGINEERING DATA

Article

pubs.acs.org/jced

Liquid−Liquid Equilibrium in *N*-Methyl-2-hydroxyethylammonium Acetate, Butanoate, or Hexanoate Ionic Liquids + Dibenzothiophene + *n*-Dodecane Systems at 298.2 K and Atmospheric Pressure

Leonardo Hadlich de Oliveira,* Víctor Hugo Álvarez,* and Martín Aznar*

School of Chemical Engineering, University of Campinas, Av. Albert Einstein 500, 13083-852 Campinas-SP, Brazil

Supporting Information

ABSTRACT: Liquid−liquid equilibrium (LLE) data are presented for ammonium based ionic liquids (ILs) + dibenzothiophene (DBT) + *n*-dodecane at 298.2 K and atmospheric pressure (~95 kPa). Mole fractions were determined by the refractometry or graphical method. DBT phase distribution, ionic liquid selectivity, and DBT percent extraction were determined. Ionic liquids used here were compared with imidazolium in terms of sulfur removal. Hand and Othmer−Tobias correlations were used to test the LLE data and gave $\sigma < 0.09$ ($R^2 > 0.90$). The nonrandom two-liquid model (NRTL) was used to correlate the LLE data, giving percent root-mean-square deviations < 0.22 between experimental and calculated mole fractions.

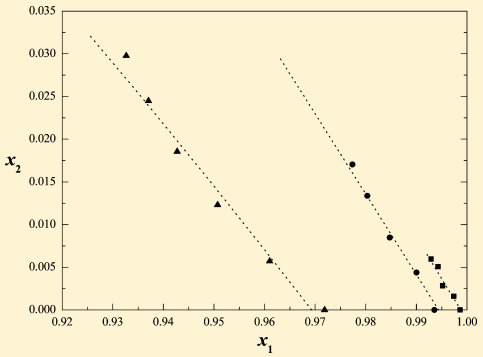

INTRODUCTION

Diesel extractive desulfurization (EDS) process involves separation of sulfur compounds from fuel using a liquid extracting agent that is not miscible with diesel. EDS generally is performed at mild operation conditions (low pressure and temperature). EDS involving ionic liquids as extracting solvents, DBT derivatives as solute sulfur species, C_{12}, or C_{16} as model diesel oil was presented previously in some works.[1−6]

According to the literature, oxidative desulfurization (ODS) seems to be a good alternative for diesel desulfurization.[7−11] This process can be combined with EDS with ionic liquids giving the called extractive and catalytic oxidative desulfurization (ECODS).[12−14] In these systems, sulfur compounds are initially extracted from model oils and then oxidized to sulfoxides and sulfones in the ionic liquid phase.

Most of EDS, ODS, and ECODS studies deal with imidazolium based ionic liquids, which have high ecological drawbacks comparing with ammonium based ionic liquids.[15,16] Considering this and joining the same background and objectives of previous works[4−6] with ECODS scope, here ammonium ionic liquids, instead of imidazolium ones, were used for extractive desulfurization of model diesel oil. In this way, LLE data were determined for the systems {*n*-methyl-2-hydroxyethylamonium acetate (m-2-HEAA) or *n*-methyl-2-hydroxyethylamonium butanoate (m-2-HEAB), or *n*-methyl-2-hydroxyethylamonium hexanoate (m-2-HEAH)} + dibenzothiophene (DBT) + *n*-dodecane at 298.2 K and atmospheric pressure (~95 kPa). The system m-2-HEAB + DBT + *n*-dodecane was presented at the XVIII Brazilian Congress of Chemical Engineering in September, 2010.[17]

Table 1. Properties of Pure Components

		n (T = 298.2 K)			
chemical	M/g mol^{-1}	exptl	lit.	purity mass fraction[a]	supplier
m-2-HEAA	135.16	1.4584	1.4494[b]	< 0.0005	
m-2-HEAB	163.215	1.4563	1.4549[b]	< 0.0005	
m-2-HEAH	191.27	1.4555		< 0.0005	
DBT	184.26			≥ 0.98	Fluka
n-dodecane	170.33	1.4196	1.42011[c]	0.996	Fluka

[a]For ionic liquids, purity is expressed in water mass fraction. [b]Reference 18. [c]Reference 3.

EXPERIMENTAL SECTION

Materials and Procedure. The properties of the chemicals used here are shown in Table 1. The ionic liquids m-2-HEAA, m-2-HEAB, and m-2-HEAH were synthesized in our laboratory according to Álvarez et al.[18] The LLE experimental procedure (cloud point method + tie-line construction) and the purification of ionic liquids, i.e., removal of residual volatile compounds and moisture, were made as reported previously,[4−6] with some added remarks as follows:

(1) For cloud points, the technique used is the well-known titration method, based in turbidimetry, and well reported by Novák et al.,[19] for binary and ternary systems. The reliability of this method is given by the added component drop mass, in addition with the mass of the

Received: July 27, 2011
Accepted: January 9, 2012
Published: February 8, 2012

   dx.doi.org/10.1021/je200799u | *J. Chem. Eng.Data* 2012, 57, 744−750

binary mixture to be titrated and refractive index measurement. In this work, we determined cloud points for ionic liquid phase only since one drop of ionic liquid did not dissolve in *n*-dodecane phase (see Uncertainty and Data Quality Tests section for detection limit of IL in alkane phase).

(2) For tie-lines, the LLE data determined are not physically in the metastable region because it is guaranteed by the long time agitation (12 h) and separation (24 h), with the formation of two clean liquid phases.

Thermodynamic Correlation. The LLE is basically determined by the $\gamma-\gamma$ approach, eq 1.

$$x_i^I \gamma_i^I = x_i^{II} \gamma_i^{II} \quad (1)$$

γ_i and x_i represent the activity coefficient and mole fraction of component i present in both phases I and II. One can use models or equations of state to calculate γ and correlate the experimental data. In this work, the nonrandom two-liquid model (NRTL)[20] was used to calculate the activity coefficient of each component in both equilibrium phases. The thermodynamic correlation was made by estimating new parameters for NRTL model, which has the following eqs:

$$\ln \gamma_i = \frac{\sum_j \tau_{ji} G_{ji} x_j}{\sum_k G_{ki} x_k} + \sum_j \frac{x_j G_{ij}}{\sum_k G_{kj} x_k}\left[\tau_{ij} - \frac{\sum_k x_k \tau_{kj} G_{kj}}{\sum_k G_{kj} x_k}\right] \quad (2)$$

$$G_{ij} = \exp(-\alpha_{ij}\tau_{ij}) \quad (\alpha_{ij} = \alpha_{ji}) \quad (3)$$

$$\tau_{ij} = \frac{\Delta g_{ij}}{RT} = A_{ij} + \frac{B_{ij}}{T} \quad (\tau_{ij} \neq \tau_{ji}) \quad (4)$$

The symbols *A*, *B*, *G*, *R*, *T*, α, τ refer to interaction energy adjustable parameter, temperature dependence interaction energy adjustable parameter, a Boltzmann-type distribution term for local composition interaction energy, ideal gas constant, temperature, mixture nonrandomness adjustable parameter, and a characteristic excess Gibbs energy parameter accounting two-body interactions. Subscripts i, j, and k refer to each component.

The model energy interaction parameters were estimated by using a procedure similar to Stragevitch and D'Ávila;[21] the nonrandomness parameter was kept constant and equal to 0.2. This estimation procedure is based on the modified Simplex method[22] and consists of the minimization of an activity-based objective function, F_a,[23] given by eq 5.

$$F_a = \sum_t^T \sum_l^L \sum_c^{C-1} [(a_{qrst}^I - a_{qrst}^{II})/(a_{qrst}^I + a_{qrst}^{II})]^2 \quad (5)$$

where *c* represents each component and *C* is the total number of components; *l* represents each tie-line in a total of *L* tie-lines; and *t* represents each temperature in a total of *T* temperatures. Calculated compositions can be compared with the experimental ones through the percent root-mean-square deviation (rmsd), δx, given by eq 6.

$$\delta x = 100\sqrt{\frac{\sum_q^Q \sum_l^L \sum_c^C (x_{clq}^{exp} - x_{clq}^{calc})^2}{2LQ}} \quad (6)$$

where superscripts exp and calc represent experimental and calculated data respectively; *q* is each phase in a total of Q phases.

RESULTS AND DISCUSSION

Cloud Points and Calibration Curves. The mass fractions *w* and refractive indices *n* of cloud points determined are presented in Table 2. The ionic liquid-rich phase binodal curves obtained from these cloud points are shown in Figure 1. An

Table 2. Cloud Points for IL (1) + DBT (2) + *n*-Dodecane (3) Systems at 298.2 K

IL	x_1	x_2	*n*
m-2-HEAA	0.9987	0.0000	
	0.9974	0.0016	
	0.9952	0.0028	
	0.9943	0.0051	
	0.9929	0.0060	
m-2-HEAB	0.9936	0.0000	1.4560
	0.9901	0.0043	1.4569
	0.9848	0.0084	1.4579
	0.9803	0.0134	1.4591
	0.9774	0.0170	1.4601
m-2-HEAH	0.9719	0.0000	1.4546
	0.9610	0.0057	1.4558
	0.9507	0.0123	1.4569
	0.9427	0.0186	1.4582
	0.9370	0.0245	1.4593
	0.9327	0.0298	1.4601

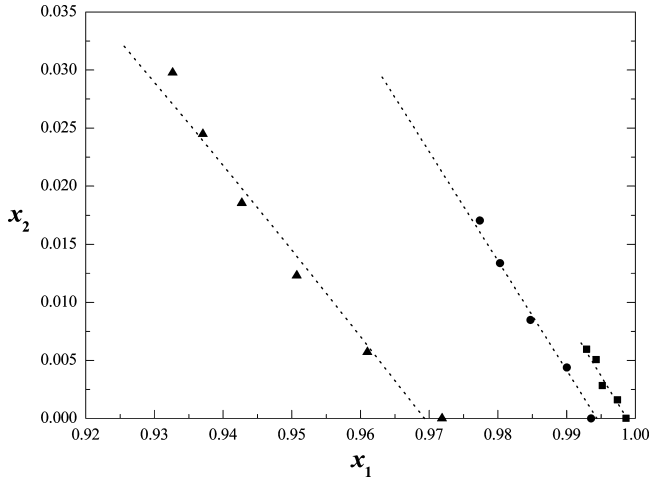

Figure 1. Experimental cloud points for ammonium ionic liquids + DBT + *n*-dodecane systems at 298.2 K: ■, m-2-HEAA; ●, m-2-HEAB; ▲, m-2-HEAH; dotted lines are calculated by NRTL.

increase in homogeneous region is observed with the increase in ionic liquid anion size, i.e., DBT and *n*-dodecane present more affinity for ammonium ionic liquids with longer chain anion. This was also observed for imidazolium ionic liquids in previous EDS researches.[24,25] Possibly, increasing the anion chain length causes an increase in aliphatic character of ionic liquid, enhancing the DBT and alkane solubilities. Distribution and selectivity data show that this effect is more pronounced for *n*-dodecane than for DBT solubility.

Calibration curves obtained from cloud points were used for composition determination of phases in equilibrium. To obtain these curves for the m-2-HEAB (1) + DBT (2) + *n*-dodecane (3) system, linear regression was performed in cloud point data

dx.doi.org/10.1021/je200799u | J. Chem. Eng.Data 2012, 57, 744–750

Table 3. LLE Data for IL (1) + DBT (2) + *n*-Dodecane (3) System at 298.2 K

	liquid−liquid equilibrium data								
	feed		IL-rich phase		alkane-rich phase				
IL	x_1	x_2	x_1	x_2	x_1	x_2	K^a	S^b	10^4u
m-2-HEAA	0.4202	0.0000	0.9987	0.0	0.0	0.0			0.0
	0.4382	0.0085	0.9973	0.0015	0.0	0.0140	0.105	86.69	0.0
	0.4318	0.0171	0.9948	0.0038	0.0	0.0272	0.140	101.02	0.0
	0.4166	0.0251	0.9946	0.0045	0.0	0.0401	0.112	112.46	0.0
m-2-HEAB	0.3684	0.0000	0.9936	0.0	0.0	0.0			0.0
	0.3787	0.0094	0.9877	0.0062	0.0	0.0128	0.487	79.37	6.6
	0.3762	0.0189	0.9828	0.0112	0.0	0.0245	0.456	74.55	4.5
	0.3749	0.0272	0.9779	0.0162	0.0	0.0353	0.459	75.27	6.0
m-2-HEAH	0.4502	0.0000	0.9719	0.0	0.0	0.0			
	0.3438	0.0097	0.9564	0.0081	0.0	0.0107	0.757	21.10	0.2
	0.3434	0.0202	0.9454	0.0161	0.0	0.0225	0.716	18.17	0.1
	0.3353	0.0303	0.9338	0.0274	0.0	0.0337	0.813	20.25	8.6

$^aK = x_2^{ilp}/x_2^{ap}$. $^bS = (x_2^{ilp}/x_2^{ap})/(x_3^{ilp}/x_3^{ap})$.

of Table 2 and gives eqs 7 and 8 for the ionic liquid-rich phase.

$$n = 1.6720 - 0.2175w_1 \quad (7)$$

$$n = 1.4559 + 0.2138w_2 \quad (8)$$

For the m-2-HEAH (1) + DBT (2) + *n*-dodecane (3) system, nonlinear (logarithm) or linear regression gives eqs 9 and 10 for the ionic liquid-rich phase.

$$n = 1.4362 - 0.0068\ln(w_1 - 0.9076) \quad (9)$$

$$n = 1.4547 + 0.1921w_2 \quad (10)$$

For the m-2-HEAA (1) + DBT (2) + *n*-dodecane (3) system, the composition determination of the m-2-HEAA rich phase was made by the graphical method described elsewhere,[6] because reliable regression eqs could not be determined for this phase due to low concentration range. The alkane phase, composed by a binary *n*-dodecane + DBT mixture was determined by the equation determined previously.[5]

Experimental Equilibrium Data. LLE data (mole fractions) for {m-2-HEAA or m-2-HEAB or m-2-HEAH} + DBT + *n*-dodecane at 298.2 K and atmospheric pressure (~95 kPa) are presented in Table 3, together with solute distribution coefficient (K) and the selectivity of the solvent (S).

Rectangular diagrams representing the LLE data are shown in Figure 2. These plots are used to better represent the LLE region that is at the bottom of a conventional triangular diagram, as pointed out by Eβer et al.[2]

The slope of the tie-lines in Figure 2 and the distribution of DBT in both phases (Figure 3) show that the solute dissolves preferably in *n*-dodecane. Selectivity values obtained here (Figure 4), compared with those reported previously,[5] lead to the fact that m-2-HEAB presents a similar behavior of [emim][$EtSO_4$], m-2-HEAA behaves between [emim][$EtSO_4$] and [emim][$DEtPO_4$], and m-2-HEAH shows the lower values. This is explained by the low solubility of *n*-dodecane relative to DBT in m-2-HEAA rich phase, as also shown by the cloud points obtained. For comparison, experimental results for [emim][$DEPO_4$] and [emim][$EtSO_4$] are also shown in Figures 3 and 4.

Uncertainty and Data Quality Tests. As mentioned, cloud points were made only for ionic liquid-rich phase since it was verified that one drop of ionic liquid does not solubilize in *n*-dodecane rich phase, e.g., the quantity of ionic liquid in *n*-dodecane phase was below the refraction detection limit ($0.4{\cdot}10^{-3}$ mol·mol^{-1}).

The mole fraction uncertainty in cloud points were derived from two sources of errors: weighing (systematic error) and titration (random error). Once the system mass was relatively high, weighing gives very low values of mole fraction uncertainty for each cloud point (approx. $\pm$ $4{\cdot}10^{-6}$); in titration, the uncertainty is associated with the drop mass added. In this work, we used a drop mass of dodecane equal to 0.0054 $\pm$ 0.0007 g and binary mixtures of 5.5975 $\pm$ 0.5335 g (average for all cloud points). Supposing that one drop of *n*-dodecane overpasses the binodal line, this gives mole fraction uncertainty values for m-2-HEAA, m-2-HEAB, and m-2-HEAH rich phases, equal to 0.0003, 0.0007, and 0.0005, respectively.

The mole fraction uncertainty in LLE data depends on refractive index measurements and the equation (calibration curve) used to obtain the respective component mole fraction. For the m-2-HEAH system, the uncertainties in ionic liquid-rich phase are < 0.0027, < 0.0002, and < 0.0028 for m-2-HEAH, DBT, and *n*-dodecane, respectively, and in alkane phase are < 0.0006 for DBT and *n*-dodecane; for the m-2-HEAB system, the uncertainties in ionic liquid-rich phase are < 0.0062 for m-2HEAB and *n*-dodecane and < 0.0002 for DBT, and in alkane phase are < 0.0008 for DBT and *n*-dodecane; for the m-2-HEAA system, the uncertainties in ionic liquid-rich phase cannot be calculated because the graphical method was applied, and in alkane phase are < 0.0006 for DBT and *n*-dodecane. The equations used to calculate the uncertainties are shown as Supporting Information.

In addition to the uncertainties calculation, two tests that can be made to verify the data quality were performed. The first is the tie-lines agreement with feed points, which indicates the experimental error by mass balance and/or analysis, and was calculated according to our previous work.[6] This value is derived from refractive index measurements and from calibration curves used to calculate each phase composition, is represented by u, and is measured in mole fraction. Table 3 shows u values obtained here, all < 0.0009.

The second test is the well-known experimental data fit by Hand[26] and Othmer−Tobias[27] correlations, eqs 11 and 12, respectively.

$$\log\left(\frac{x_2^{ilp}}{x_1^{ilp}}\right) = s_H \log\left(\frac{x_2^{ap}}{x_3^{ap}}\right) + i_H \quad (11)$$

dx.doi.org/10.1021/je200799u | J. Chem. Eng.Data 2012, 57, 744−750

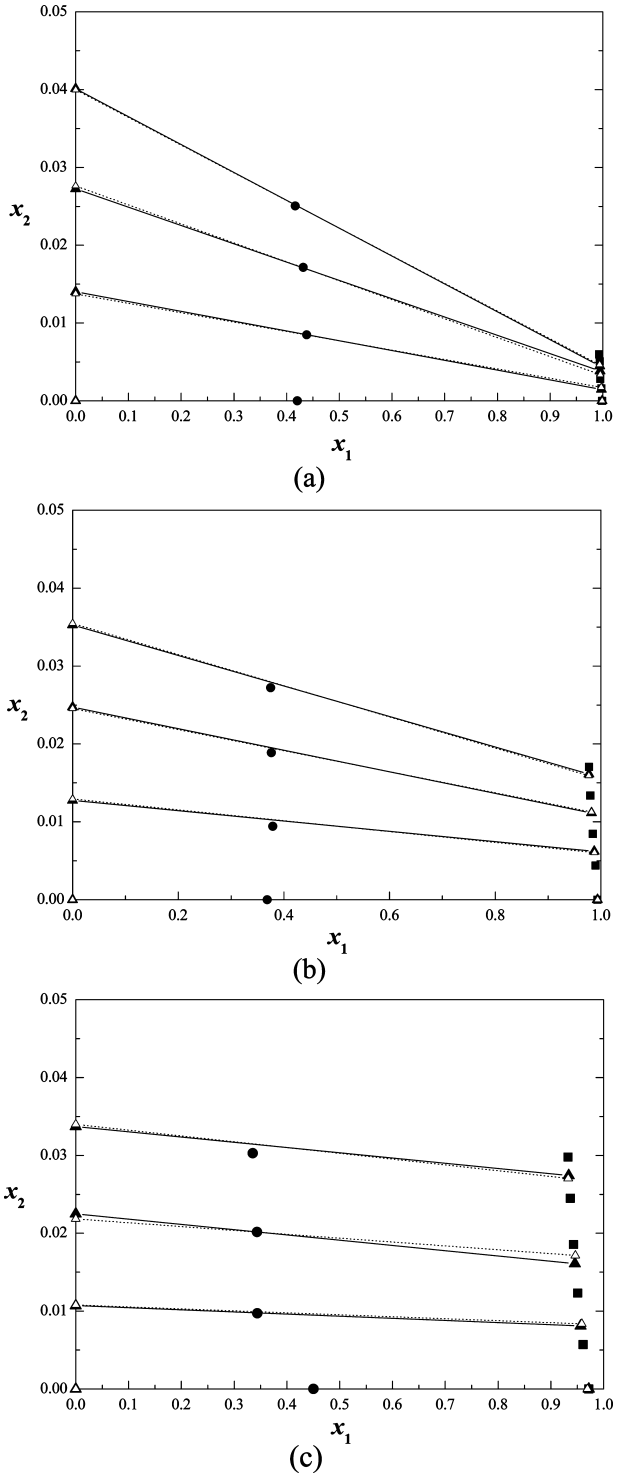

Figure 2. Experimental and calculated LLE data for ammonium ionic liquids + DBT + *n*-dodecane at 298.2 K: (a) m-2-HEAA; (b) m-2-HEAB; (c) m-2-HEAH; ■, cloud points; ●, feed points; ▲, solid line, tie-lines; Δ, dotted line, NRTL correlation.

$$\log\left(\frac{1-x_1^{ilp}}{x_1^{ilp}}\right) = s_{OT}\log\left(\frac{1-x_3^{ap}}{x_3^{ap}}\right) + i_{OT} \quad (12)$$

In eqs 11 and 12, *s* and *i* are the slope and the intercept of Hand and Othmer−Tobias linear equations. $R^2 > 0.90$ and

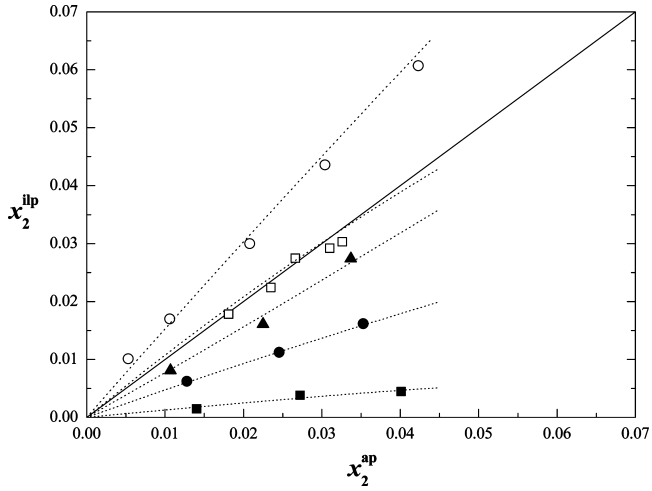

Figure 3. Distribution of DBT between ionic liquid and alkane rich phase at 298.2 K: ■, m-2-HEAA; ●, m-2-HEAB; ▲, m-2-HEAH; □, [emim][$EtSO_4$];[5] ○, [emim][$DEtPO_4$];[5] dotted lines are calculated by NRTL.

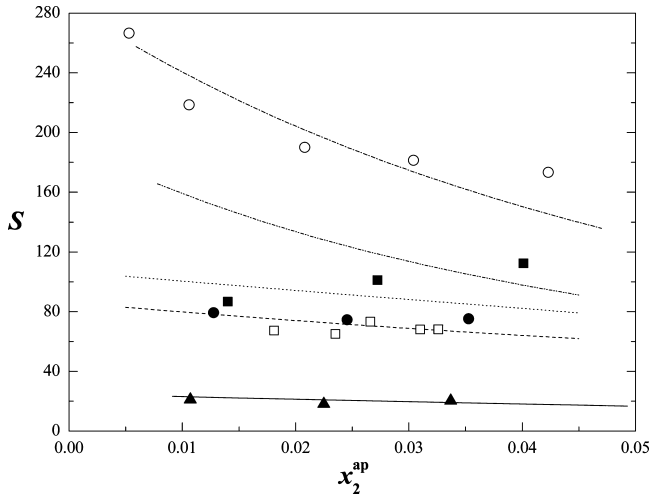

Figure 4. Selectivity of ionic liquids at 298.2 K: ■ and dotted line, m-2-HEAA; ● and dashed line, m-2-HEAB; ▲ and solid line, m-2-HEAH; □ and dash-dot-dot line, [emim][$EtSO_4$];[5] ○ and dash-dot line, [emim][$DEtPO_4$];[5] lines are calculated by NRTL.

$\sigma < 0.09$ was obtained for both correlations, as shown in Table 4 and Figure 5, which represent a good linear fit.

NRTL Parameters. The estimation of NRTL parameters made in this work used, as input information, LLE data for ionic liquid + aromatic sulfur compound + n-dodecane LLE determined previously by Oliveira and Aznar[4−6] together with the new LLE data obtained here. This action generalizes the binary interaction parameters for all these systems. Also, B_{ij} (and B_{ji}) were set equal to 0, avoiding a forced linear temperature dependence of the parameters and increasing the degrees of freedom of the correlation. α_{ij} was set equal to 0.2 by the same reason. So, 63 tie lines (12 obtained in this work) were correlated with 34 parameters.

All estimated parameters are shown in Table 5, and the calculated results are shown in Figure 1 to 4. In Figures 1 to 3, the NRTL model shows good approximations for the experimental results; in Figure 4, the model correlates well low selectivities values for the systems treated here. For comparison, NRTL results for [emim][$DEPO_4$] and [emim][$EtSO_4$] are

dx.doi.org/10.1021/je200799u | J. Chem. Eng.Data 2012, 57, 744−750

Table 4. Hand[a] and Othmer–Tobias[b] Linear Equations Slopes, Intercepts, Linear Coefficients of Determination (R^2),[c] and Standard Deviations (σ) for Systems Studied in This Work

Hand				Othmer–Tobias			
s_H	i_H	R^2	σ_H	s_H	i_H	R^2	σ_{OT}
m-2-HEAA (1) + DBT (2) + dodecane (3)							
1.0777	−0.8144	0.9417	0.0897	0.6995	−1.2591	0.9047	0.0760
m-2-HEAB (1) + DBT (2) + dodecane (3)							
0.9258	−0.4553	0.9991	0.0090	0.5668	−0.8394	0.9937	0.0146
m-2-HEAH (1) + DBT (2) + dodecane (3)							
1.0448	−0.0285	0.9911	0.0360	0.3694	−0.6198	0.9845	0.0169

[a]From eq 11. [b]from eq 12. [c]Mole fraction range of validity: from the lower to the upper ternary tie-line composition.

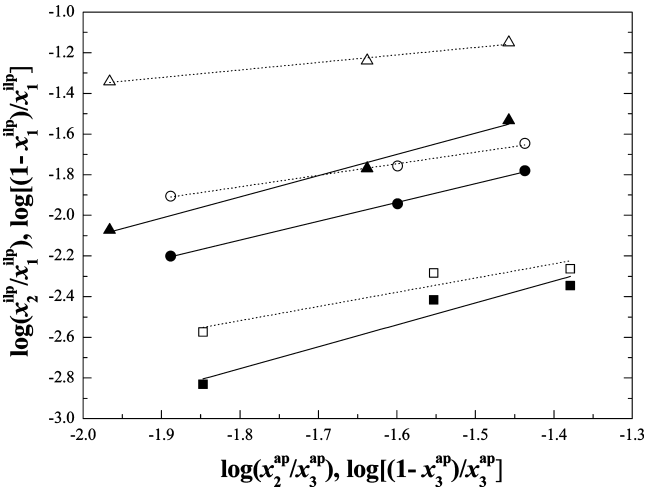

Figure 5. Hand (full symbols) and Othmer–Tobias (open symbols) plots for IL + DBT + *n*-dodecane systems studied here at 298.2 K: ■, m-2-HEAA; ●, m-2-HEAB; ▲, m-2-HEAH.

Table 5. Estimated NRTL Parameters (A_{ij}, A_{ji}) and Root-Mean-Square Deviations (δx)[a]

i	j	A_{ij}	A_{ji}
DBT (1), 4-MDBT (2), 4,6-DMDBT (3), *n*-dodecane (4), [emim][DEtPO$_4$] (5), [emim][EtSO$_4$] (6), m-2-HEAA (7), m-2-HEAB (8), m-2-HEAH (9), δx = 0.0022			
1	**4**	**−176.25**	**653.66**
1	5	88.313	257.12
1	6	3298.1	83.670
1	**7**	**−255.36**	**1375.4**
1	**8**	**71.638**	**625.28**
1	**9**	**−29.522**	**640.14**
2	4	−105.55	366.83
2	5	1053.4	−220.86
2	6	1773.3	19.617
3	4	3887.5	−1955.6
3	5	−3906.3	−3200.5
3	6	1159.8	−1318.8
4	5	1944.6	1052.9
4	6	4612.7	1365.2
4	**7**	**4557.6**	**1799.5**
4	**8**	**2562.7**	**1099.1**
4	**9**	**5055.4**	**979.21**

[a]$\alpha_{ij} = \alpha_{ji}$ was kept constant and equal to 0.2. $B_{ij} = B_{ji} = 0$. The values in bold were used to obtain the calculated tie-lines for the systems treated in this work. The other values generalize the previous ones estimated in other works.[4−6]

also shown in Figures 3 and 4, and can show that this parameter generalized NRTL, does not give good results for [emim][EtSO$_4$] or m-2-HEAA selectivity. Root mean square deviations below 0.0306, 0.0323, and 0.1205 were achieved for each m-2-HEAA, m-2-HEAB, and m-2-HEAH system, respectively. A δx < 0.2197 were achieved for all 63 tie lines.

Removal of DBT. The analysis for DBT extraction percent (E) was made by the liquid–liquid equilibrium data presented in Table 3 and eqs 13 to 15.[6] An ionic liquid/*n*-dodecane mass ratio = 0.6 was used to obtain the data presented here.

$$E = \frac{C_0 - C_f}{C_0} \times 100 \tag{13}$$

Table 6. DBT Extraction Percent of Each Ionic Liquid at 298.2 K

IL	C_0	E
m-2-HEAA	0.0163	7.3
	0.0325	9.7
	0.0463	6.6
m-2-HEAB	0.0164	15.7
	0.0326	18.8
	0.0469	18.9
m-2-HEAH	0.0160	27.8
	0.0332	26.9
	0.0491	25.9

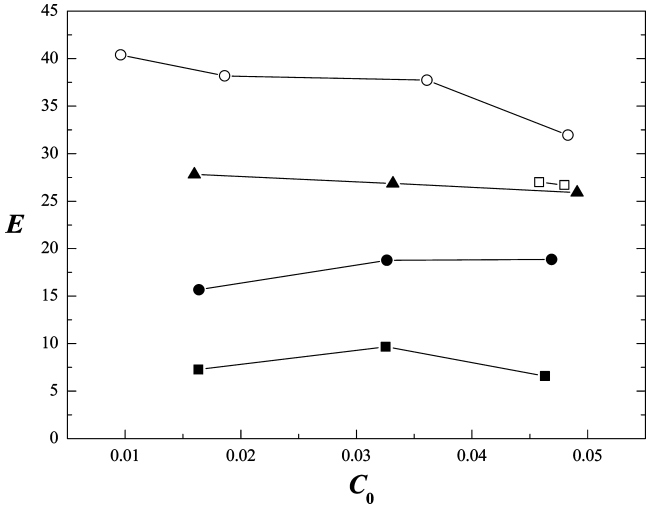

Figure 6. DBT extraction percent at 298.2 K: ■, m-2-HEAA; ●, m-2-HEAB; ▲, m-2-HEAH; □, [emim][EtSO$_4$];[5] ○, [emim][DEtPO$_4$].[5]

dx.doi.org/10.1021/je200799u | J. Chem. Eng.Data 2012, 57, 744–750

$$C_0 = \left(\frac{w_2}{w_2 + w_3}\right)_{\text{feed}} \quad (14)$$

$$C_f = \left(\frac{w_2}{w_2 + w_3}\right)_{\text{alkane phase}} \quad (15)$$

In eqs 13 to 15, C_0 and C_f are the mass fractions of DBT in dodecane before and after equilibrium, respectively. The extraction results are shown in Table 6 and Figure 6. For systems with m-2-HEAA, the percent of DBT extraction was below 10 %; with m-2-HEAB, the values are between (15 and 20) %; and for m-2-HEAH, between (25 and 30) %.

Comparing *K*, *S*, and *E* values obtained here with those obtained for [emim][$EtSO_4$] and for [emim][$DEtPO_4$],[5] m-2-HEAH presents potential to substitute these imidazolium ionic liquids, mainly [emim][$EtSO_4$]. Moreover, m-2-HEAH is cheaper to produce and more green to the environment.

CONCLUSIONS

Phase diagrams showing experimental liquid−liquid equilibrium data were obtained for the {m-2-HEAA or m-2-HEAB or m-2-HEAH} + DBT + *n*-dodecane system at 298.2 K and ∼95 kPa. From these data, the following conclusions can be made:

(1) These ammonium ionic liquids did not dissolve in *n*-dodecane in concentrations greater than $0.4 \cdot 10^{-3}$ mol·mol^{-1}.
(2) The one phase region, DBT partition, and extraction percent increase in the order: m-2-HEAA < m-2-HEAB < m-2-HEAH.
(3) Ionic liquid selectivities increase in the inverse order.
(4) Enhancing the size of the anion increases more *n*-dodecane solubility than DBT solubility in ionic liquids used here.
(5) Data quality was ascertained by uncertainty calculation, mass balance, and Hand and Othmer−Tobias eqs.
(6) NRTL models were used for all desulfurization systems studied by our group until now and shows percent rmsd below 0.0022 for the systems treated here.

ASSOCIATED CONTENT

Supporting Information

Uncertainty calculation for cloud points and LLE data. This material is available free of charge via the Internet at http://pubs.acs.org.

AUTHOR INFORMATION

Corresponding Author

* (L.H.d.O) Tel: +55 19 3521 3896. E-mail: leonardoh.deoliveira@gmail.com. (V.H.M.) E-mail: mister_alvarez@hotmail.com. (M.A.) Tel: +55 19 3521 3962. E-mail: maznar@feq.unicamp.br.

Funding

The financial support from FAPESP (grants 07/53024-3 and 07/52032-2) is gratefully acknowledged. M.A. is the recipient of a CNPq fellowship.

REFERENCES

(1) Zhang, S.; Zhang, Q.; Zhang., Z. C. Extractive desulfurization and denitrogenation of fuels using ionic liquids. *Ind. Eng. Chem. Res.* **2004**, *43*, 612−622.
(2) Eβer, J.; Wasserscheid, P.; Jess, A. Deep desulfurization of oil refinery streams by extraction with ionic liquids. *Green Chem.* **2004**, *6*, 316−322.
(3) Alonso, L.; Arce, A.; Francisco, M.; Soto, A. Thiophene separation from aliphatic hydrocarbons using the 1-ethyl-3-methylimidazolium ethylsulfate ionic liquid. *Fluid Phase Equilib.* **2008**, *270*, 97−102.
(4) Oliveira, L. H.; Aznar, M. Liquid−liquid equilibrium data in ionic liquid + 4-methyldibenzothiophene + *n*-dodecane systems. *Ind. Eng. Chem. Res.* **2010**, *49*, 9462−9468.
(5) Oliveira, L. H.; Aznar, M. Phase equilibria in ionic liquids + dibenzothiophene + *n*-dodecane systems. *Ind. Eng. Chem. Res.* **2011**, *50*, 2289−2295.
(6) Oliveira, L. H.; Aznar, M. Liquid−liquid equilibria for {1-ethyl-3-methylimidazolium diethylphosphate or 1-ethyl-3-methylimidazolium ethylsulfate} + 4,6-dimethyldibenzothiophene + dodecane systems at 298.2 and 313.2 K. *J. Chem. Eng. Data* **2011**, *56*, 2005−2012.
(7) Te, M.; Fairbridge, C.; Ring, Z. Oxidation reactivities of dibenzothiophenes in polyoxometalate/H_2O_2 and formic acid/H_2O_2 systems. *Appl. Catal., A* **2001**, *219*, 267−280.
(8) Campos-Martin, J. M.; Capel-Sanchez, M. C.; Fierro, J. L. G. Highly efficient deep desulfurization of fuels by chemical oxidation. *Green Chem.* **2004**, *6*, 557−562.
(9) Al-Shahrani, F.; Xiao, T.; Llewellyn, S. A.; Barri, S.; Jiang, Z.; Shi, H.; Martinie, G.; Green, M. L. H. Desulfurization of diesel via the H_2O_2 oxidation of aromatic sulfides to sulfones using a tungstate catalyst. *Appl. Catal., B* **2007**, *73*, 311−316.
(10) Xu, D.; Zhu, W.; Li, H.; Zhang, J.; Zou, F.; Shi, H.; Yan, Y. Oxidative desulfurization of fuels catalyzed by V_2O_5 in ionic liquids at room temperature. *Energy Fuels* **2009**, *23*, 5929−5933.
(11) Zhang, W.; Xu, K.; Zhang, Q.; Liu, D.; Wu, S.; Verpoort, F.; Song, X.-M. Oxidative desulfurization of dibenzothiophene catalyzed by ionic liquid [BMIm]HSO_4. *Ind. Eng. Chem. Res.* **2010**, *49*, 11760−11763.
(12) He, L.; Li, H.; Zhu, W.; Guo, J.; Jiang, X.; Lu, J.; Yan, Y. Deep oxidative desulfurization of fuels using peroxophosphomolybdate catalysts in ionic liquids. *Ind. Eng. Chem. Res.* **2008**, *47*, 6890−6895.
(13) Li, H.; He, L.; Lu, J.; Zhu, W.; Jiang, X.; Wang, Y.; Yan, Y. Deep oxidative desulfurization of fuels catalyzed by phosphotungstic acid in ionic liquids at room temperature. *Energ. Fuel.* **2009**, *23*, 1354−1357.
(14) Li, H.; Jiang, X.; Zhu, W.; Lu, J.; Shu, H.; Yan, Y. Deep oxidative desulfurization of fuel oils catalyzed by decatungstates in the ionic liquid of [Bmim]PF_6. *Ind. Eng. Chem. Res.* **2009**, *48*, 9034−9039.
(15) Zhao, D.; Liao, Y.; Zhang, Z. Toxicity of ionic liquids. *Clean* **2007**, *35*, 42−48.
(16) Pham, T. P. T; Cho, C.-W.; Yun, Y.-S. Environmental fate and toxicity of ionic liquids: A review. *Water Res.* **2010**, *44*, 352−372.
(17) Oliveira, L. H.; Álvarez, V. H.; Aznar, M. Liquid−liquid Equilibrium for *n*-dodecane + DBT + *N*-methyl-2-hydroxiethylammonium Butyrate at 25°C and 95 kPa. *XVIII Brazilian Congress of Chemical Engineering*, Foz do Iguaçu, Brazil, **2010**.
(18) Álvarez, V. H.; Dosil, N.; Gonzalez-Cabaleiro, R.; Mattedi, S.; Martin-Pastor, M.; Iglesias, M.; Navaza, J. M. Brønsted ionic liquids for sustainable processes: synthesis and physical properties. *J. Chem. Eng. Data* **2010**, *55*, 625−632.
(19) Novák, J. P.; Matous, J.; Pick, J. *Liquid−Liquid Equilibrium*; Elsevier: Amsterdam, 1987.
(20) Renon, H.; Prausnitz, J. M. Local compositions in thermodynamic excess functions for liquid mixtures. *AIChE J.* **1968**, *14*, 135−144.
(21) Stragevitch, L.; d'Avila, S. G. Application of a generalized maximum likelihood method in the reduction of multicomponent liquid−liquid equilibrium data. *Braz. J. Chem. Eng.* **1997**, *14*, 41−52.
(22) Nelder, J. A.; Mead, R. A Simplex method for function minimization. *Comput. J.* **1965**, *7*, 308−313 1965.
(23) Sørensen, J. M.; Magnussen, T.; Rasmussen, P.; Fredenslund, A. Liquid−liquid equilibrium data: their retrieval, correlation and prediction. Part II: correlation. *Fluid Phase Equilib.* **1979**, *3*, 47−82.

(24) Bösmann, A.; Datsevich, L.; Jess, A.; Lauter, A.; Schmitz, C.; Wasserscheid, P. Deep desulfurization of diesel fuel by extraction with ionic liquids. *Chem. Commun.* **2001**, 2494−2495.
(25) Jiang, X.; Nie, Y.; Li, C.; Wang, Z. Imidazolium-based alkylphosphate ionic liquids: a potential solvent for extractive desulfurization of fuel. *Fuel* **2008**, *87*, 79−84.
(26) Hand, D. B. Dineric distribution. *J. Phys. Chem.* **1930**, *34*, 1961−2000.
(27) Othmer, D. F.; Tobias, P. E. Tie-line correlation. *Ind. Eng. Chem.* **1942**, *34*, 693−696.